

Slow-fast dynamics of Hopfield spruce-budworm model with memory effects

Na Wang Maoan Han

Hefei University

2016. 6. 26

- 1 Introduction
- 2 The model equation
- 3 Slow-fast dynamics
- 4 Numerical example

In this study we analyze the following spruce budworm system of equations

$$\begin{cases} \dot{N}(t') = rN(t')\left(1 - \frac{N(t')}{kS(t')}\right) - \beta \frac{P(N(t'))^2}{\eta^2(S(t'))^2 + (N(t'))^2}, \\ \dot{S}(t') = \rho S(t')\left(1 - \frac{\int_{-\infty}^{t'} W(t'-z)S(z)dz}{S_{max}}\right) - \delta N(t'). \end{cases} \quad (1.1)$$

where k and S_{max} are the effective carrying capacity coefficient for budworm and spruce respectively, β and δ are two different timescale of budworm and spruce respectively, P is the maximal loss of budworm due to higher order predators, η is the effective regulation coefficient for the predation pressure.

The distributed delay represented by the weight function $W(s) : R^+ \rightarrow R^+$ satisfies $W(s) \geq 0$ and $\int_0^\infty W(t)dt = 1$. In this paper $W(s)$ defined by

$$W(s) = a^2 s e^{-as}, \quad a > 0, \quad (1.2)$$

which is term as the so-called strong generic kernel function (memory with hump) and is a particular case of the Gamma Function described by Fargue. The "strong" generic kernel implies that a particular time in the past is more important than any other.

★ By means of a change of variables, we first transform system (31) with the strong delay kernel into a four-dimensional system of differential equations.

★ By linearizing the resulting four-dimensional system at the positive equilibrium and analyzing the associated characteristic equation, the Hopf bifurcations are demonstrated. In particular, by applying geometric singular perturbation theory, the approximate expression of the relaxation oscillation and its period are obtained analytically.

★ To verify our theoretical predictions, two numerical simulations are also included in part three.

We define two new variables as

$$Q(t') = \int_{-\infty}^{t'} W(t' - z)S(z)dz = a^2 \int_{-\infty}^{t'} (t' - z)S(z)e^{-a(t'-z)} dz,$$

and

$$R(t') = a \int_{-\infty}^{t'} S(z)e^{-a(t'-z)} dz.$$

We have

$$\begin{cases} \varepsilon \frac{dZ}{d\tau} = YF_0\left(\frac{Z}{Y}, Y; \alpha^2\right), \\ \frac{dY}{d\tau} = Yf\left(\frac{Z}{Y}, V; \varrho, Y_{max}\right), \\ \frac{dV}{d\tau} = f^*(V, U; a), \\ \frac{dU}{d\tau} = g^*(Y, U; a), \end{cases} \quad (2.1)$$

Remark 1: The model with the delay kernel $W(s)$ is very hard to analyze. So authors use many methods to eliminate delay. By defining new variables and using the linear chain trick technique, the original model can be rewritten as the equivalent systems (2.1) without delay. But the price is the dimension of equations would be increased from two to four. Although the model becomes to the four-dimensional system (2.1), the variables U and V of the systems do not play a major role. Therefore, we only need to analyze the first two equations of (2.1).

where

$$\begin{aligned}F_0(X, Y; \alpha^2) &= X(1 - X) - \frac{1}{Y} \cdot \frac{X^2}{\alpha^2 + X^2}, \\f(X, V; \varrho, Y_{max}) &= 1 - \frac{V}{Y_{max}} - \varrho X, \\f^*(V, U; a) &= a(U - V), \\g^*(Y, U; a) &= a(Y - U),\end{aligned}$$

and $0 < \varepsilon \ll 1$.

Introduce a fast time variable $t = \frac{\tau}{\varepsilon}$, and denote $Z(t) = Z(\varepsilon t)$, $Y(t) = Y(\varepsilon t)$, $V(t) = V(\varepsilon t)$ and $U(t) = U(\varepsilon t)$, then Eq. (2.1) becomes

$$\begin{cases} \frac{dZ}{dt} = YF_0\left(\frac{Z}{Y}, Y; \alpha^2\right), \\ \frac{dY}{dt} = \varepsilon Yf\left(\frac{Z}{Y}, V; \varrho, Y_{max}\right), \\ \frac{dV}{dt} = \varepsilon f^*(V, U; a) \\ \frac{dU}{dt} = \varepsilon g^*(Y, U; a). \end{cases} \quad (2.2)$$

Let $\varepsilon \rightarrow 0$ in Eq. (2.2), one has a fast subsystem governing the fast variable only

$$\frac{dZ}{dt} = YF_0\left(\frac{Z}{Y}, Y; \alpha^2\right), \quad (2.3)$$

where Y is regarded as a parameter.

Firstly, the geometric singular perturbation theory defines the slow manifold of Eq. (2.2) as the equilibria of the fast subsystem Eq. (2.3)

$$\begin{aligned} M &= \left\{ (Z, Y, V, U) \mid YF_0\left(\frac{Z}{Y}, Y; \alpha^2\right) = 0 \right\}, \\ &= \left\{ (Z, Y, V, U) \mid Y = \frac{X}{(\alpha^2 + X^2)(1 - X)} \right\}, \end{aligned} \quad (3.1)$$

where $X = \frac{Z}{Y}$.

In the following discussion, the case with δ -shape curve of the slow manifold is focused on, correspondingly, let α^2 satisfy $0 < \alpha^2 < \frac{1}{27}$ (see Fig.1).

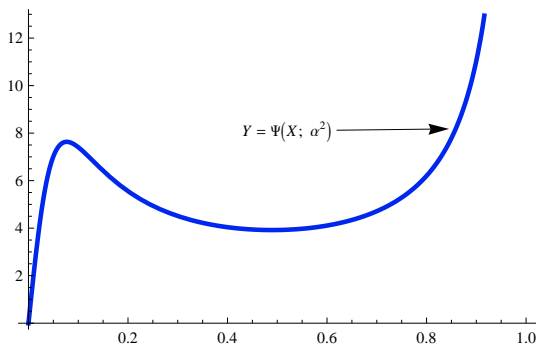


Fig.1 The case with δ -shape curve of the slow manifold with the Projection on (X, Y) plane.

For any equilibrium point (Y_0, X_0) , the linearized system is

$$\frac{dZ}{dt} = \left[1 - 2X_0 - \frac{2\alpha^2 X_0}{Y_0(\alpha^2 + X_0^2)^2} \right] Z(t). \quad (3.2)$$

In the slow manifold M , the one eigenvalue of Eq. (3.2) is

$$\lambda = 1 - 2X_0 - \frac{2\alpha^2 X_0}{Y_0(\alpha^2 + X_0^2)^2}.$$

As for λ , there are two critical points X_1 and X_2 satisfy with $0 < X_1 < \frac{1}{3} < X_2 \leq \frac{1}{2} < 1$ such that $\lambda > 0$ with $X_0 \in (X_1, X_2)$ and $\lambda < 0$ with $X_0 \in (0, X_1) \cup (X_2, 1)$.

And the slow manifold M is divided into three parts by the bifurcation points B_1 and B_2

$$M = M_1 + M_2 + M_3.$$

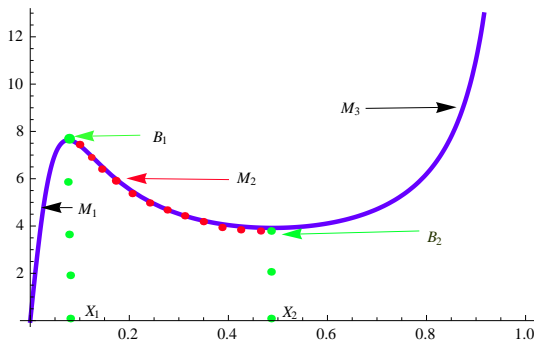


Fig.2 The structure of the slow manifold M of Eq. (2.2) with the Projection on (X, Y) plane, where B_1 and B_2 are the saddle-node bifurcation points.

Next, we consider the location and stability of the equilibrium points of Eq. (2.2).

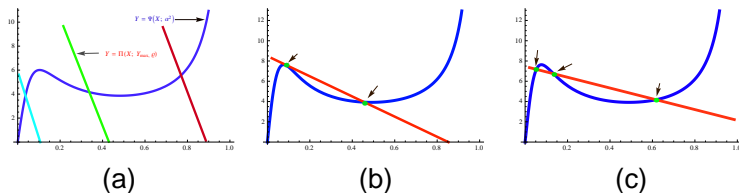


Fig.3 Different cases of the number and location of the equilibrium points of Eq. (2.2) with the Projection on (X, Y) plane.

To decide the stability of those equilibrium points, consider the characteristic equation

$$D(\lambda) = \lambda^4 + b\lambda^3 + c\lambda^2 + d\lambda + e = 0. \quad (3.3)$$

where

$$b = \varepsilon(2a - \rho X_0),$$

$$c = \varepsilon(a^2 + \rho X_0 - \rho X_0^2) - \varepsilon^2 \cdot 2a\rho X_0,$$

$$d = \varepsilon^2 \left[a\rho X_0(2 - 2X_0 - a) + \frac{a^2 Y_0}{Y_{max}} \right],$$

$$e = \varepsilon^2 a^2 \rho X_0(1 - X_0).$$

Thus, when the equilibrium point $(Z_0, Y_0, V_0, U_0) \in M_2$ and $\varrho > \frac{2a}{X_0}$ or $\varrho X_0(2 - 2X_0 - a) + \frac{aY_0}{Y_{max}} < 0$, then those equilibrium points locate in M_2 is unstable. When the equilibrium point $(Z_0, Y_0, V_0, U_0) \in M_1 \cup M_3$ and the proper adjustment of ϱ , Y_{max} and a satisfy with $\varrho < \frac{2a}{X_0}$ and $\varrho X_0(2 - 2X_0 - a) + \frac{aY_0}{Y_{max}} > 0$, then those equilibrium points locate in $M_1 \cup M_3$ are stable.

Remark 2: The original model in reference [A Rasmussen, J Wyller, J O Vik] is a 2D system. The authors used $tr(J)$ and $det(J)$ to judge the positive and negative of eigenvalues. However, the corresponding characteristic equation of our model is a quartic equation. Thus, the positive and negative judgment of eigenvalues is more complicated. Through the analysis of characteristic equation, the positive and negative of characteristic roots was obtained.

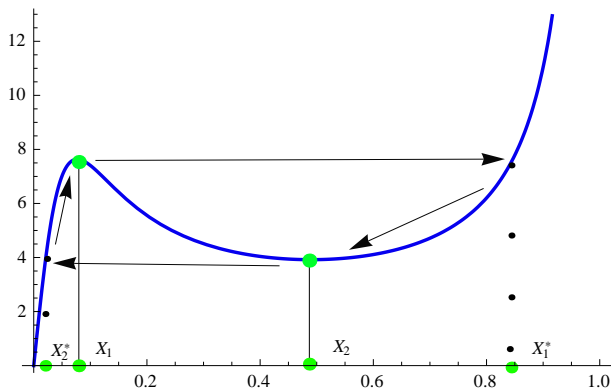


Fig.4 The relaxation oscillation of Eq. (2.2) with the Projection on (X, Y) plane.

Remark 3: Reference [A Rasmussen, J Wyller, J O Vik] used the attraction domain of the upper and lower stable branch of the quasi-steady state to judge the the clockwise direction of the relaxation oscillation. In this paper, we used sign of $\frac{dY}{d\tau}$ to judge the the clockwise direction of the the relaxation oscillation. This method is more simple and clear in comparison.

The relaxation oscillation of (1.1) is described approximately as

$$\left\{ \begin{array}{ll} Y = \frac{X}{(X^2 + \alpha^2)(1 - X)}, & X \in (X_2^*, X_1], \\ Z = Y_1 X_1, & X \in (X_1, X_1^*], \\ Y = \frac{X}{(X^2 + \alpha^2)(1 - X)}, & X \in [X_2, X_1^*), \\ Z = Y_2 X_2, & X \in [X_2^*, X_2), \end{array} \right. \quad (3.4)$$

where $\frac{X_i^*}{((X_i^*)^2 + \alpha^2)(1 - X_i^*)} = Y_i^*$.

$$\begin{aligned}
T &= \int_{M_1} d\tau + \int_{M_3} d\tau + O(\varepsilon) \\
&\approx \int_{M_1} \frac{dY}{Yf(X, V; \varrho, Y_{max})} + \int_{M_3} \frac{dY}{Yf(X, V; \varrho, Y_{max})} \\
&= \int_{X_2^*}^{X_1} \frac{\Psi'(X)dX}{\Psi(X)f(X, \Psi(X); \varrho, Y_{max})} + \int_{X_2}^{X_1^*} \frac{\Psi'(X)dX}{\Psi(X)f(X, \Psi(X); \varrho, Y_{max})} \\
&= Y_{max} \left(\int_{X_2^*}^{X_1} \frac{\mathbb{P}_3(X)dX}{X\mathbb{P}_4(X)} + \int_{X_1^*}^{X_2} \frac{\mathbb{P}_3(X)dX}{X\mathbb{P}_4(X)} \right), \tag{3.5}
\end{aligned}$$

where $\mathbb{P}_4(X) = Y_{max}\varrho X^4 - Y_{max}(1 + \varrho)X^3 + Y_{max}(1 + \alpha^2\varrho)X^2 - (1 + \alpha^2Y_{max} + \alpha^2\varrho Y_{max})X + \alpha^2Y_{max}$.

Proposition If one of the following two conditions is hold

$$(H_1) \max\left\{\frac{1}{X_2}, \frac{2a}{X_2}, \frac{2a}{X_1}\right\} < \varrho < \frac{1}{X_1}, \quad -Y_{max}\varrho < -\frac{Y_1}{X_2 - X_1};$$

$$(H_2) \frac{1}{X_2} < \varrho < \frac{1}{X_1}, \quad -Y_{max}\varrho < -\frac{Y_1}{X_2 - X_1} \text{ and } \varrho X_i(2 - 2X_i - a) + \frac{aY_i}{Y_{max}} < 0 (i = 1, 2),$$

then the predator-prey system undergoes relaxation oscillation, and the analytical expressions of the relaxation oscillation and its period are described approximatively as Eqs. (3.4) and (3.5) respectively.

Remark 4: Conditions H_1 and H_2 are incompatible.

Example 1. Let $\varepsilon = 0.001$, $\alpha^2 = 0.0085$, $Y_{max} = 16$, $\varrho = 5.5$, $a = 0.2$, Eq.(2.2) reads

$$\begin{cases} \frac{dZ}{dt} = Y \left[X(1 - X) - \frac{1}{Y} \cdot \frac{X^2}{0.0085 + X^2} \right], \\ \frac{dY}{dt} = \varepsilon Y \left(1 - \frac{V}{16} - 5.5X \right), \\ \frac{dV}{dt} = 0.2\varepsilon(U - V), \\ \frac{dU}{dt} = 0.2\varepsilon(Y - U), \end{cases} \quad (4.1)$$

where $X = \frac{Z}{Y}$.

By calculating on the platform of **Mathematica**, we have

$X_1 = 0.103536$, $X_2 = 0.481682$, $Y_1 = 6.00913$, $Y_2 = 3.86382$,
 $X_1^* = 0.792927$, $X_2^* = 0.0366351$, $\frac{1}{X_2} = 2.07606$, $\frac{1}{X_1} = 9.65845$. It is
 easy to see that $\max\{\frac{1}{X_2}, \frac{2a}{X_2}, \frac{2a}{X_1}\} < \varrho = 5.5 < \frac{1}{X_1}$, $-Y_{max\varrho} = -88$
 $< -\frac{Y_1}{X_2 - X_1} = -15.891$. The system undergoes relaxation oscillation,
 this result is confirmed by the numerical result in Fig.5.

From Eq. (3.4), the approximate expression of the relaxation oscillation is

$$\left\{ \begin{array}{ll} Y = \frac{X}{(X^2 + \alpha^2)(1 - X)}, & X \in (0.0366351, 0.103536], \\ Z = 0.622161, & X \in (0.103536, 0.792927], \\ Y = \frac{X}{(X^2 + \alpha^2)(1 - X)}, & X \in [0.481682, 0.792927), \\ Z = 1.86113, & X \in (0.0366351, 0.489569). \end{array} \right. \quad (4.2)$$

From Eq.(3.5), one obtains the approximate period of the relaxation oscillation $T_{appr} = 1.4124$, which agrees with the numerical result $T = 1.76242$.

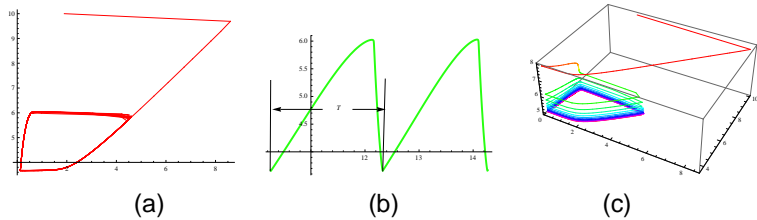


Fig.5 The relaxation oscillation of Eq. (4.1).

Example 2. Let $\varepsilon = 0.001$, $\alpha^2 = 0.0085$, $Y_{max} = 32$, $\varrho = 4$, $a = 3.7$, Eq.(2.2) reads

$$\begin{cases} \frac{dZ}{dt} = Y \left[X(1 - X) - \frac{1}{Y} \cdot \frac{X^2}{0.0085 + X^2} \right], \\ \frac{dY}{dt} = \varepsilon Y \left(1 - \frac{V}{32} - 4X \right), \\ \frac{dV}{dt} = 3.7\varepsilon(U - V), \\ \frac{dU}{dt} = 3.7\varepsilon(Y - U), \end{cases} \quad (4.3)$$

where $X = \frac{Z}{Y}$.

Since $\frac{1}{X_2} < \varrho = 4 < \frac{1}{X_1}$, $-Y_{max}\varrho = -128 < -\frac{Y_1}{X_2 - X_1} = -15.891$,
 $\varrho X_1(2 - 2X_1 - a) + \frac{aY_1}{Y_{max}} = -0.0949968 < 0$ and $\varrho X_2(2 - 2X_2 - a)$
 $+ \frac{aY_2}{Y_{max}} = -4.68482 < 0$, the system undergoes relaxation oscillation.
 This result is confirmed by the numerical result in Fig.6. From
 Eq.(3.5), one obtains the approximate period of the relaxation
 oscillation $T_{appr} = 0.94409$, which agrees with the numerical result
 $T = 1.05677$.

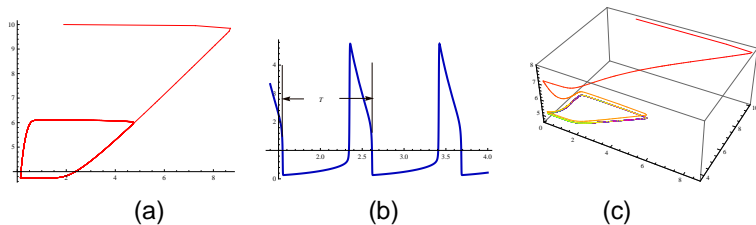


Fig.6 The relaxation oscillation of Eq. (4.3).

Remark 5: Though the two phase planes look very similar for the two cases, they represent two different cases which satisfied incompatible conditions H_1 and H_2 .

- ▶ model (1.1) with delay kernel
→ system (2.2) without delay
- ▶ slow manifold M

$\left\{ \begin{array}{l} \textit{shape} \\ \textit{stability} \\ \textit{bifurcation} \\ \textit{location and stability of the equilibrium point} \end{array} \right.$

- ▶ Proposition

Thank you!